

BOSE-EINSTEIN CORRELATIONS AND THE EQUATION OF STATE OF NUCLEAR MATTER IN RELATIVISTIC HEAVY-ION COLLISIONS

B. R. Schlei

*Physics Division P-25, Los Alamos National Laboratory, Los Alamos,
NM 87545, USA*

E-mail: schlei@LANL.gov

Experimental spectra of the CERN/SPS experiments NA44 and NA49 are fitted while using four different equations of state of nuclear matter within a relativistic hydrodynamic framework. For the freeze-out temperatures, $T_f = 139$ MeV and $T_f = 116$ MeV, respectively, the corresponding freeze-out hypersurfaces and Bose-Einstein correlation functions for identical pion pairs are discussed. It is concluded, that the Bose-Einstein interferometry measures the relationship between the temperature and the energy density in the equation of state of nuclear matter at the late hadronic stage of the fireball expansion. It is necessary, to use the detailed detector acceptances in the calculations for the Bose-Einstein correlations.

1 Introduction

The equation of state (EOS) of nuclear matter at very high energy densities is heretofore unknown. Many observables have been proposed as a signature for a possible new state of nuclear matter, i.e., the quark-gluon plasma (QGP), which could be formed within the very hot and dense zones of nuclear matter – the fireballs – in relativistic heavy-ion collision experiments. Among the proposed signatures for a QGP are Bose-Einstein correlations (BEC), which are correlations of identical hadron pairs. BEC functions are sensitive to the space-time dynamics of the fireball and therefore should give clues about the EOS, which governs the evolution of those fireballs.

Among the many scientific contributions on BEC (for a recent overview, *cf.*, the book by Weiner¹) only few of them (*cf.*, e.g., Rischke *et al.*²) address the particular role of the EOS of nuclear matter in the intensity interferometry of identical hadrons, i.e., BEC. It is the purpose of this paper to further investigate the interplay between the EOS and BEC. In the following, we shall consider a framework of analysis which is based on relativistic hydrodynamics, because this approach allows for an explicit use of an EOS.

In order to address the issues raised above, we shall use the simulation code HYLANDER-C³ with different equations of state and Cooper-Frye⁴ freeze-out. Experimental single particle momentum distributions from 158A GeV Pb+Pb collisions, measured by the NA44^{5,6} and NA49⁷ Collaborations, are used as fit criteria for the hydrodynamical (one-fluid-type) calculations.

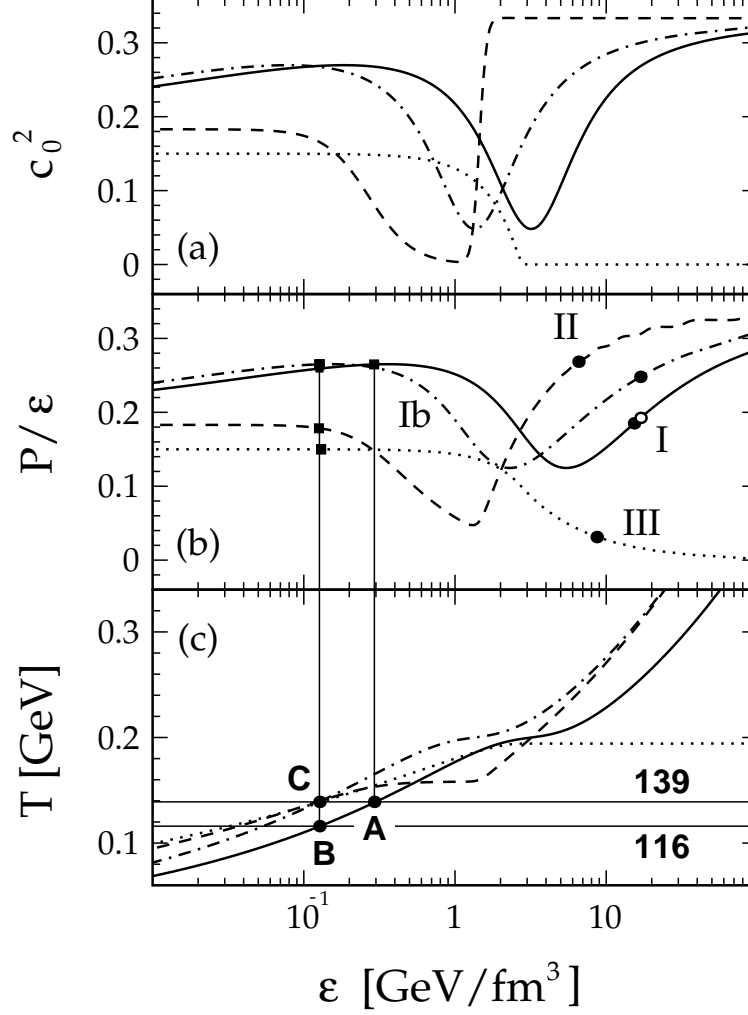


Figure 1: Speed of sound, c_0^2 , ratio of pressure and energy density, P/ϵ , and temperature, T , as functions of ϵ , for the equations of state EOS-I (solid lines), EOS-II (dashed lines), EOS-III (dotted lines), and EOS Ib (dashed-dotted lines), respectively. The dots in plot (b) correspond for each EOS to the starting values of P/ϵ with respect to the achieved initial maximum energy density ϵ_Δ at transverse position $r_\perp = 0$, (dots correspond to $T_f = 139$ MeV whereas the open circle corresponds to $T_f = 116$ MeV). The squares indicate the final values of P/ϵ at breakup energy densities, ϵ_f . The dots A, B, C in plot (c) indicate the relationship between the temperature and the energy density at the late hadronic stage of the fireball expansion.

After a discussion of the space-time features of the particular fireballs we shall compare BEC of identical pion pairs to experimental correlation functions, which have been measured by NA44⁸.

2 The Equations of State of Nuclear Matter

In the hydrodynamic approach, virtually any type of EOS can be considered when solving the relativistic Euler-equations⁹. The coupled system of partial differential equations necessary that describe the dynamics of a relativistic fluid (with given initial conditions) contains an equation of state which we write in the form

$$P(\epsilon, n) = c^2(\epsilon, n) \epsilon. \quad (1)$$

In Eq. (1), the quantities P , ϵ , and n are the pressure, the energy density, and the baryon density, respectively. The proportionality constant, c^2 , is in general a function of ϵ and n . In the following, we shall assume that in particular the n dependence is negligible for the energy regime under consideration. From only the knowledge of the speed of sound, $c_o^2(\epsilon)$, one can then calculate $c^2(\epsilon)$ by solving the integral¹⁰

$$c^2(\epsilon) = \frac{1}{\epsilon} \int_0^\epsilon c_o^2(\epsilon') d\epsilon'. \quad (2)$$

Assuming an adiabatic expansion, the temperature, $T(\epsilon)$, can be calculated from¹⁰

$$T(\epsilon) = T_0 \exp \left[\int_{\epsilon_0}^\epsilon \frac{c_o^2(\epsilon') d\epsilon'}{(1 + c^2(\epsilon')) \epsilon'} \right], \quad (3)$$

where $T_0 = T(\epsilon_0)$ has to be specified for an arbitrary value of ϵ_0 .

The first equation of state¹¹, EOS-I, which we use in the following exhibits a phase transition to a quark-gluon plasma at a critical temperature $T_c = 200$ MeV with a critical energy density $\epsilon_c = 3.2$ GeV/fm³. The second equation of state¹², EOS-II, is also a lattice QCD-based EOS which has recently become very popular in the field of relativistic heavy-ion physics. This equation of state includes a phase transition to a quark-gluon plasma at $T_c = 160$ MeV with a critical energy density $\epsilon_c \approx 1.5$ GeV/fm³. The third equation of state, EOS-III, has been extracted from the microscopic transport model RQMD¹³ under the assumption of complete thermalization, and does *not* include a transition to a QGP. We obtain a fourth equation of state, EOS-Ib, by changing the relationship between ϵ_c and T_c in EOS-I to $T_c(\epsilon_c = 1.35$ GeV/fm³) = 200 MeV.

In Fig. 1 the four equations of state are plotted in many different representations. The particular parametrizations for the speed of sound which have been used here are published in Schlei *et al.*¹⁰.

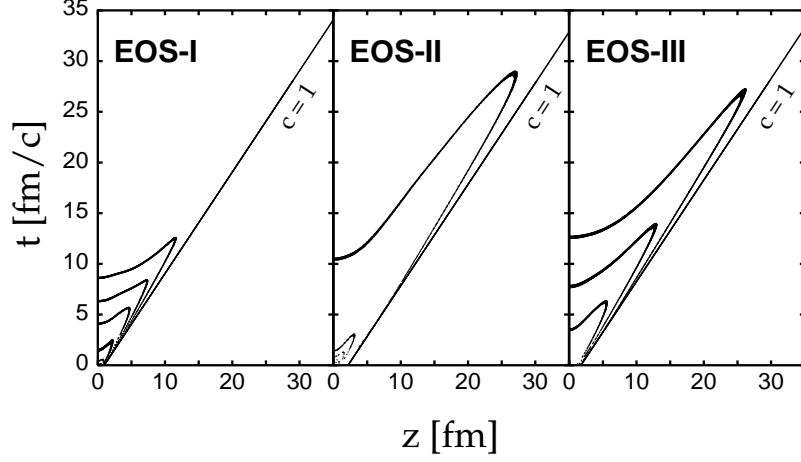


Figure 2: Isothermes for the relativistic fluids governed by EOS-I, EOS-II and EOS-III at $r_{\perp} = 0$, respectively. The outer lines correspond to a temperature, $T = 140 \text{ MeV}$, and each successively smaller curve represents a reduction in temperature by $\Delta T = 20 \text{ MeV}$. The lines $c = 1$ represent the light cone.

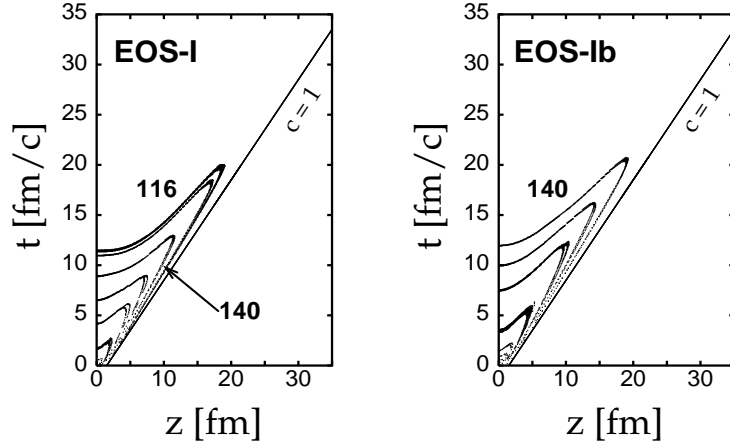


Figure 3: Isothermes for the relativistic fluids governed by EOS-I, and EOS-Ib at $r_{\perp} = 0$, respectively. For EOS-I the lines (beginning with the most outer curves) correspond to temperatures, $T = 116 \text{ MeV}$, 120 MeV , 140 MeV , 160 MeV ... etc. For EOS-Ib, the outer lines correspond to a temperature, $T = 140 \text{ MeV}$, and each successively smaller curve represents a reduction in temperature by $\Delta T = 20 \text{ MeV}$. The lines $c = 1$ represent the light cone.

3 Fits to Experimental Spectra and Freeze-Out

In the following, we shall discuss five scenarios: we compare four calculations using EOS-I, EOS-II, EOS-III, and EOS-Ib for the fixed freeze-out temperature, $T_f = 139 \text{ MeV}$, and one calculation using EOS-I for the fixed freeze-out temperature, $T_f = 116 \text{ MeV}$.

In particular, it is assumed that due to an experimental uncertainty for the centrality of the collision, only 90% of the total available energy and the total baryon number have been observed. It is then possible to find initial distributions for the four equations of state, such that one can reproduce the single inclusive momentum spectra of 158 AGeV Pb+Pb collisions. For a freeze-out temperature, $T_f = 139 \text{ MeV}$, the initial conditions and a large number of final single inclusive momentum distributions for various hadron species have been published in Schlei *et al.*^{3,10} in comparison to the data measured by the NA44^{5,6} and NA49⁷ Collaborations. The so far published results refer to calculations using EOS-I, EOS-II, and EOS-III. Results showing the fits of single inclusive particle momentum spectra using EOS-Ib with $T_f = 139 \text{ MeV}$ and EOS-I with $T_f = 116 \text{ MeV}$ will be published elsewhere¹⁴.

It should be stressed, that all here discussed calculations result in single particle momentum distributions, which describe the corresponding data to the same extent very well. Although EOS-II was found in the calculations of hadronic transverse mass spectra to be too soft (*cf.* Schlei *et al.*^{3,10}), we shall use it here also for the calculation of Bose-Einstein correlation functions. Before we discuss BEC, we have to discuss briefly the thermal evolution of the various fireballs.

Figs. 2 and 3 show isothermes for the relativistic Pb+Pb fluids governed by the different equations of state until freeze-out has been reached. The calculation using EOS-I with $T_f = 139 \text{ MeV}$ leads to a fireball of a much shorter lifetime than the calculations using EOS-II and EOS-III with $T_f = 139 \text{ MeV}$. This behaviour is caused by much smaller freeze-out energy densities, ϵ_f , in the calculations using EOS-II and EOS-III compared to the calculation using EOS-I. We have $\epsilon_f = 0.292 [0.126 (0.130)] \text{ GeV}/fm^3$ when using EOS-I [EOS-II (EOS-III)]. A fluid that undergoes adiabatic expansion needs more time to reach the smaller freeze-out energy densities.

Since EOS-II and EOS-III yield similar lifetimes of the fireball, in the following we attempt to increase the lifetime of the system which is governed by EOS-I. This can be achieved by (a) using a smaller freeze-out temperature, $T_f = 116 \text{ MeV}$, or (b) by hardening the EOS, i.e., using EOS-Ib instead of EOS-I (without changing $T_f = 139 \text{ MeV}$). For the latter two cases, we obtain $\epsilon_f = 0.127 \text{ GeV}/fm^3$ (*cf.* Fig. 1 (c) and Fig. 3).

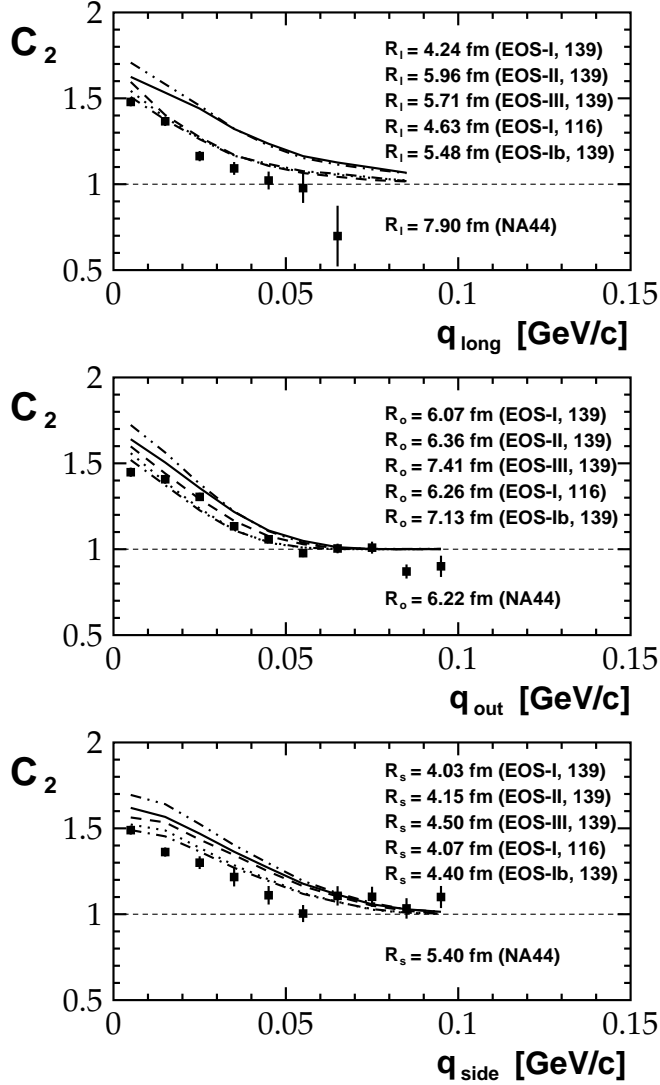


Figure 4: Projections of BEC functions for $\pi^+\pi^+$ pairs emerging from the low p_\perp (horizontal and vertical) acceptance setting of the NA44 detector⁸. The data points are data taken by the NA44 Collaboration⁸. The solid [dashed [dotted [dashed-dotted]]] lines correspond to the calculations using EOS-I [EOS-II [EOS-III [EOS-Ib]]] with $T_f = 139$ MeV, and the double dotted-dashed lines correspond to the calculation using EOS-I with $T_f = 116$ MeV. The values of the inverse width parameters, R_i ($i = l, o, s$), have been obtained from the Gaussian Bertsch-Pratt parametrization (see text).

4 Bose-Einstein Correlations

The lifetime of the fireball is, e.g., reflected in Bose-Einstein correlations of identical pion pairs¹⁵. Within the Bertsch-Pratt variables¹⁶, a very sensitive quantity – regardless of whether one is interested in transverse expansion¹⁷ and BEC, or in the role of resonance decay¹⁸ in BEC – has always been the longitudinal projection of the two-pion correlation function, $C_2(q_{long})$. Fig. 4 shows projections of BEC functions for $\pi^+\pi^+$ pairs emerging from the low p_\perp (horizontal and vertical) acceptance setting of the NA44 detector⁸. The data points are data taken by the NA44 Collaboration⁸.

It must be stressed, that in the calculations it was necessary to fully simulate the experimental detector acceptance. I have checked, that if one *does not follow* the experimental prescription in generating the correlation functions one could obtain errors for the inverse widths and the overall strengths of the correlation functions in the order of 25%.

Consistent with the expectation, the calculations using EOS-II, EOS-III, and EOS-Ib give similar lifetimes and therefore sufficiently large longitudinally expanded fireballs (see Figs. 2,3). In particular, these calculations give – in addition to the excellent description^{3,10,14} of hadronic single inclusive momentum spectra (except for EOS-II) – a very nice reproduction of the pionic NA44 BEC data. It should be stressed here, that a freeze-out temperature $T_f = 139$ MeV was *sufficient* to achieve this agreement.

Also consistent with expectation is that the calculation using EOS-I with $T_f = 139$ MeV gave a too small longitudinally expanded fireball (see above, and Fig. 2). On the contrary, it is on first sight surprising that a reduction of the freeze-out temperature to $T_f = 116$ MeV does not lead to large enough longitudinal extension of the fireball in the calculation which uses EOS-I. The reason for this result is the following: a freeze-out temperature reduction leads to a larger lifetime of the *direct* fireball, but the relative fraction of present resonance decay contributions is reduced (by about 30%); i.e., the resonance halo is reduced in size. Hence, the *total* fireball, which is a superposition of the direct (or thermal) fireball and the resonance halo remains moreless unchanged in size.

In conclusion, by inspecting Fig. 1(c) we can see that only those equations of state which go through point *C* in the figure reproduce the experimental data on Bose-Einstein correlations good enough. Changing the freeze-out temperature shows hardly any effect. Therefore, the measurements of Bose-Einstein correlations tell us about which relationship between temperature and energy density is necessary for a valid choice of an equation of state in the calculations. Unfortunately, from the above made considerations it must be noted,

that two-particle BEC *seen by itself* cannot be used as a tool to determine a possible phase-transition to a QGP, because the BEC show no sensitivity to the structure of the EOS.

Acknowledgments

I would like to thank the organizers for their invitation to present these results at the “Correlations and Fluctuations '98” workshop in Mátraháza, Hungary. In particular, I am grateful for discussions with Drs. D. Strottman and M. Gyulassy. Special thanks goes to Drs. J.P. Sullivan and H.W. van Hecke for explaining and providing the NA44 Bose-Einstein data to me. This work has been supported by the U.S. Department of Energy.

References

1. R.M. Weiner, ”Bose-Einstein Correlations in Particle and Nuclear Physics - A Collection of Reprints”, John Wiley & Sons (1997).
2. D.H. Rischke, M. Gyulassy, *Nucl. Phys. A* **608**, 479 (1996); S. Bernard, D.H. Rischke, J.A. Maruhn, W. Greiner, *Nucl. Phys. A* **625**, 473, (1997).
3. B.R. Schlei, *Heavy Ion Phys.* **5**, 403 (1997).
4. F. Cooper, G. Frye, E. Schonberg, *Phys. Rev. D* **11** 192 (1975).
5. Nu Xu for the NA44 Collaboration, *Nucl. Phys. A* **610**, 175c (1996).
6. I.G. Bearden et al. (NA44 Collaboration), *Phys. Lett. B* **388**, 431 (1996).
7. P.G. Jones and the NA49 Collaboration, *Nucl. Phys. A* **610**, 188c (1996).
8. I.G. Bearden et al. (NA44 Collaboration), “High energy Pb+Pb collisions viewed by pion interferometry”, *Phys. Rev. C*, (1998), in print.
9. L.D. Landau, E.M. Lifschitz, “Fluid mechanics” (Pergamon, New York, 1959).
10. B.R. Schlei, D. Strottman, and N. Xu, *Phys. Rev. Lett.* **80**, 3467 (1998).
11. K. Redlich, H. Satz, *Phys. Rev. D* **33**, 3747 (1986).
12. C.M. Hung, E.V. Shuryak, *Phys. Rev Lett.* **75** 4003 (1995).
13. H. Sorge, *Phys. Lett. B* **402**, 251 (1997).
14. B.R. Schlei, D. Strottman, J.P. Sullivan, H.W. van Hecke, in preparation.
15. B.R. Schlei, *Phys. Rev. C* **55**, 954 (1997).
16. G. Bertsch, M. Gong, and M. Tohyama, *Phys. Rev. C* **37**, 1896 (1988).
17. B.R. Schlei, U. Ornik, M. Plümer, R.M. Weiner, *Phys. Lett. B* **293**, 275 (1992).
18. J. Bolz, U. Ornik, M. Plümer, B.R. Schlei, R.M. Weiner, *Phys. Rev. D* **47**, 3860 (1993).